Åbo Akademi

OPEN ACCESS

This is an electronic reprint of the original article. This reprint may differ from the original in pagination and typographic detail.

One-pot myrtenol amination over Au, Au–Pd and Pd nanoparticles supported on alumina

S. Demidova, Yu; L. Simakova, I.; Estrada, M.; Beloshapkin, S.; V. Suslov, E.; P. Volcho, K.; F. Salakhutdinov, N.; Simakov, A.; Murzin, Dmitry

Published in:
Catalysis Letters

DOI:
10.1007/s10562-019-02958-6

Published: 01/01/2019

Document Version
Accepted author manuscript

Document License
CC BY-ND

Link to publication

Please cite the original version:
S. Demidova, Y., L. Simakova, I., Estrada, M., Beloshapkin, S., V. Suslov, E., P. Volcho, K., F. Salakhutdinov, N., Simakov, A., & Murzin, D. (2019). One-pot myrtenol amination over Au, Au–Pd and Pd nanoparticles supported on alumina. *Catalysis Letters*, *149*(12), 3454–3464. https://doi.org/10.1007/s10562-019-02958-6

General rights
Copyright and moral rights for the publications made accessible in the public portal are retained by the authors and/or other copyright owners and it is a condition of accessing publications that users recognise and abide by the legal requirements associated with these rights.

Take down policy
If you believe that this document breaches copyright please contact us providing details, and we will remove access to the work immediately and investigate your claim.

This document is downloaded from the Research Information Portal of ÅAU: 03. May. 2024

One-pot myrtenol amination over Au, Au-Pd and Pd nanoparticles supported on alumina

Yu.S. Demidova[1,2], I.L. Simakova[1,2*], M. Estrada[3], S. Beloshapkin[4], E.V. Suslov[5], K.P. Volcho[2,5], N.F. Salakhutdinov[2,5], A. Simakov[3], D.Yu. Murzin[6]

[1]*Boreskov Institute of Catalysis, pr. Lavrentieva, 5, 630090, Novosibirsk, Russia*

[2]*Novosibirsk State University, Pirogova 2, 630090, Novosibirsk, Russia*

[3]*Universidad Nacional Autónoma de México, Centro de Nanociencias y Nanotecnología, km. 107 carretera Tijuana a Ensenada, C.P. 22860, Ensenada, Baja California, México*

[4]*Bernal Institute, University of Limerick, V94 T9PX, Limerick, Ireland*

[5]*Novosibirsk Institute of Organic Chemistry, pr. Lavrentieva, 9, 630090, Novosibirsk, Russia*

[6]*Process Chemistry Centre, Åbo Akademi University, FI-20500, Turku/Åbo, Finland*

[*]E-mail: simakova@catalysis.ru

ABSTRACT

One-pot bio-based myrtenol amination was studied in the presence of alumina supported Au, Au-Pd and Pd nanoparticles subjected to the thermal treatment under oxidizing or reducing atmosphere. Myrtenol amination with aniline was carried out under nitrogen atmosphere (9 bar) at 453K using toluene as a solvent. The effect of the active metal along with the influence of redox pre-treatment on the catalytic behavior in the hydrogen borrowing reaction was explored. The catalyst characterization was done by transmission electron microscopy, X-ray photoelectron spectroscopy, inductively coupled plasma optical emission spectroscopy, nitrogen adsorption. The active metal and the catalysts redox pretreatment affected more noticeably selectivity to the reaction products rather than myrtenol conversion. Monometallic Au/Al_2O_3 catalyst promoted predominantly formation of the target secondary amine and the corresponding imine without a significant impact of the side reaction of C=C bond hydrogenation in myrtenol, whereas monometallic Pd catalyst activated C=C bond resulting in its hydrogenation. At the

same time in the presence of Au-Pd simultaneous hydrogenation of both C=C and C=N bond occurred. Au-Pd catalysts activated in oxygen and hydrogen showed different catalytic activity determined by the composition of surface active sites. Monometallic gold catalyst was more effective in the hydrogen transfer in the case of substrates with competitive unsaturated functional groups.

Keywords: alcohol amination, one-pot, hydrogen borrowing, redox treatment effect, gold, palladium, bimetallic catalyst, myrtenol, terpenoids, biomass

1. Introduction

Catalytic one-pot alcohol amination proceeding through the hydrogen borrowing process (Figure 1) is an effective approach in producing valuable amines for fine chemical synthesis and chemical industry. However, a one-pot process involving multiple catalytic reactions allows an increase of the process efficiency only when the catalytic properties in the complex catalytic system are optimized. Complexity of the one-pot alcohol amination determines a variety of parameters that can affect the catalytic performance [1-5]. In the case of complex substrates the control on the side reactions should be performed as well.

Synthesis of terpene amines is of great interest for the development of new pharmaceuticals [6-9]. Terpenoinds are the largest group of natural compounds that are extensively applied in the food and perfumery industry as flavors, fragrances and spices. At the same time high reactivity of terpenoids can lead to insufficient selectivity in various transformations of terpenoids over heterogeneous catalysts [3, 10-20]. Thus in the case of complex terpenoids it is important to control impact of side reactions in their transformations to achieve reasonable selectivity to the desired product.

In our previous work it was shown that gold catalysts exhibited good catalytic activity in one-pot bio-based myrtenol amination (Figure 2) along with a low impact of side reactions such as hydrogenation of the reactive C=C group of myrtenol by hydrogen formed in the first step [3, 16].

The influence of the support nature and gold catalysts redox pre-treatment on the catalytic activity and selectivity in myrtenol amination was explored in detail [3, 4], revealing the key parameters determining catalytic performance in this reaction. A certain balance between acid and base sites was shown to be required for the efficient one-pot alcohol amination that can be tuned by the support nature or/and preliminary catalyst activation [3, 4]. According to the plausible reaction mechanism the basic sites on metal oxide surfaces are required for the initial

alcohol activation, while the availability of protonic groups was suggested to be important for hydrogen transfer and therefore for the target amine formation [3, 21-24].

In this study to enhance fundamental understanding of one-pot alcohol amination in terms of the role of catalyst active sites as well as to optimize hydrogen transfer, the doped gold catalysts with Pd were studied [25, 26, 27]. Optimization of the hydrogen transfer is related to alcohol dehydrogenation involving metal nanoparticles and resulting in hydrogen formation followed by selective C=N bond hydrogenation of imine. Note that it was clearly demonstrated that alcohol dehydrogenation to carbonyl compound can occur both in the presence and absence of gold nanoparticles, while hydrogen formation was observed only in the presence of gold [3, 28, 29]. Alcohol dehydrogenation proceeding only on the support active sites led to inability to produce hydrogen species for further hydrogenation.

A series of alumina supported Au, Au-Pd and Pd catalysts subjected to activation in oxygen and hydrogen was studied in one-pot myrtenol amination. Based on our previous results alumina was selected as a support providing an adequate catalytic performance in terms of activity, allowing also comprehensive characterization by a range of physical-chemical techniques [3]. Note that while zirconia was shown to be an optimal catalyst for myrtenol amination the catalyst characterization faced certain difficulties particularly in the case of bimetallic systems [3].

2. Experimental/methodology

2.1. Preparation of catalysts

The catalysts tested in the current paper were synthesized similar to the procedure described in [30]. Briefly, gold (2.8 wt.% according to ICP analysis) was deposited on alumina (Sigma Aldrich) by deposition-precipitation technique using $HAuCl_4$ (Alfa-Aesar) as a gold precursor and urea (Sigma Aldrich) as a precipitating agent. 4 g of alumina were suspended in 400 ml of $HAuCl_4$(1.6×10^{-3} M) and of urea (0.42 M). The initial pH of the formed aqueous

suspension was *ca.* 2. Then the mixture was kept at 80ºC under vigorous stirring for 4 h. In order to remove the excess of chloride after gold deposition, the sample was washed with a 25 M solution of NH_4OH (pH *ca.* 10), as in [31]. Thereafter the sample was washed with deionized water, filtered and dried at room temperature for 24 h. $Au(OH)_3/Al_2O_3$ prepared in this way was used for subsequent synthesis of both Au/Al_2O_3 and $Au\text{-}Pd/Al_2O_3$ catalysts. Palladium containing catalysts, Pd/Al_2O_3 and $Au\text{-}Pd/Al_2O_3$, (0.2 wt. Pd % according to ICP analysis) were obtained by deposition of of Pd species on alumina or on alumina with previously deposited gold hydroxide using $PdCl_2$ (Alfa-Aesar) in an aqueous solution slightly acidified with HCl. Obtained suspensions were stirred for 12 h at room temperature followed by filtration and washing with ammonium hydroxide to remove chloride ions similar to the catalyst containing only gold on alumina.. Subsequent treatment included washing with water until pH 7, filtering and drying at room temperature for 24 h. Before catalytic tests, the samples were reduced in hydrogen or oxidized in air flow under a temperature increase to 350ºC with a ramp rate of 20ºC/min. The samples treated in oxygen have TPO in their code, while in hydrogen treated one were coded as sample-TPR.

2.2. Characterization of supports and catalysts

The gold and palladium content in the synthesized catalysts was analyzed with an inductively coupled plasma atomic emission spectroscopy (ICP-AES) using a Varian Liberty 110 ICP Emission Spectrometer.

The porous structure of the catalysts was evaluated by nitrogen adsorption in a Micromeritics TriStar II-3020 device. Prior the analysis, the samples were degassed in vacuum at 300°C for 4h using a Micromeritics VacPrep 061-Sample degas system. The value of specific surface area was estimated by the BET model, while the pore size distribution was determined by the BJH model.

The mean size, morphology and elements distribution for supported nanoparticles were determined by STEM using a JEOLJEM-2100F microscope with an XMAX OXFORD detector. EDX analysis for Au and Pd was performed using the INCA software. Prior to analysis, the samples were ultrasonically deposited from a suspension in propan-2-ol on a copper grid coated with carbon film. The mean diameter was evaluated via measuring more than 150 particles. The mean diameter (d_m) of particles was calculated using the following equation: $d_m = \frac{\sum_i (x_i d_i)}{\sum_i x_i}$, where x_i is the number of particles with diameter d_i.

XPS was performed using a Kratos AXIS 165 spectrometer with a monochromatic AlKα radiation (hv = 1486.58 eV) and a fixed analyzer pass energy of 20 eV. All measured binding energies (BE) were referred to the C1s line of adventitious carbon at 284.8 eV. Spectra deconvolution was carried out with the background estimated via the Shirley method.

2.3. Catalytic experiments

Liquid-phase myrtenol amination was performed in a stainless steel reactor (150 ml), equipped with an electromagnetic stirrer (1100 rpm) and the sampling system. In a typical experiment, a mixture of myrtenol (1 mmol), aniline (1 mmol) and the powdered catalyst (92 mg) in toluene (10 ml) was intensively stirred at 180°C under N_2 atmosphere (9 bar). During the course of the reaction the samples aliquots were withdrawn periodically from the reactor and analyzed by gas chromatography. Maximally 5 samples were taken with the volume *ca.* 0.1-0.2 ml each being thus in total 0.5-1 ml or 5-10 vol. % from the initial volume of the substrate solution. The reaction mixture was taken together with the catalyst under stirring and then filtered. In this way there was a negligibly influence of sampling on the catalyst bulk density.

The measurements of catalytic activity were performed in the kinetic regime. The impact of internal diffusion was determined through estimation of the Weisz–Prater criterion. The

impacts of external diffusion and mass transfer limitations through the liquid–solid interface were evaluated by the corresponding criterion calculation [16].

2.4. Product analysis

Aliquots were withdrawn from the reactor at appropriate time intervals and analyzed by gas chromatography using SLB-5ms column (length 30 m, inner diameter 0.25 mm and film thickness 0.25 μm) and a flame ionization detector operating at 300°C. Additionally the chemical nature of the products were confirmed by gas chromatography mass spectrometery (Agilent Technologies 7000 GC/MS Triple Quad, HP-5MS column) as well as ^{1}H- and ^{13}C-NMR (*Bruker DRX-500* spectrometer). NMR and GC/MS data of the products are presented in our previous work [1].

Elemental composition of the reaction products was determined by mass spectra data recorded on a *DFS Thermo Scientific* spectrometer in a full scanning mode in the range 0-500 *m/z*, ionization by electron impact 70 eV with a direct sample insertion.

Selectivity was calculated based on the following equation: selectivity = (yield of the product)/(total yield of all products). The initial reaction rate was calculated within the linear part of the kinetic curves.

3. Results and discussion

3.1. Catalysts characterization

Prior to the catalytic tests a series of Au, Au-Pd and Pd catalysts subjected to activation in oxygen and hydrogen was characterized by nitrogen adsorption, STEM, XPS and ICP. The metal content based on ICP data are presented in Table 1.

According to nitrogen adsorption the specific surface area and average pore diameter for alumina were found to be 136 m^2/g and 5.2 nm, respectively. The deposition of gold or gold-

palladium nanoparticles did not affect significantly the value of specific surface area, being 125 and 130 m^2/g, respectively.

According to TEM data the gold and gold-palladium nanoparticles are characterized with almost semispherical shape practically without well detectable crystallographic planes (Figure 3). A uniform and narrow distribution of gold metal particles both for monometallic and bimetallic catalysts was observed, being practically independent on the type of the sample pre-treatment (Table 1, Figure 3). The gold particles size was 2.6 and 2.4 nm for monometallic Au/Al_2O_3 catalyst pre-treated under oxidizing and reducing atmospheres, respectively. The bimetallic $AuPd/Al_2O_3$ catalyst exhibited gold particles sizes of 2.5 and 2.7 nm for pre-oxidized and pre-reduced samples, respectively. The presence of palladium on the surface of gold nanoparticles in case of $AuPd/Al_2O_3$ was confirmed by STEM-EDS technique (Figure 3f). The profile for palladium coincides well with that for gold across Au-Pd nanoparticles (Figure 3f). Exact location of Pd cannot be revealed based on EDS analysis. In particular Figure 3f does not allow to unequivocally conclude if the Pd signal is sufficiently above the baseline noise level in the EDS line scan. Moreover, the signal levels of Au and Pd are similar. Nevertheless, a stepwise strategy of Pd deposition on the catalyst already bearing Au and a relatively mild thermal treatment procedure allow to propose that Pd species are efficiently localized in the subsurface layer on the Au nanoparticles. Deposition of palladium onto gold nanoparticles practically did not affect the size of bimetallic nanoparticles because of a low palladium loading. Note the Pd clusters with size less than 0.3-0.4 nm are not detectable under the used TEM imaging conditions. Presence of palladium particles with the sizes larger than 0.3 nm (resolution of the measurements) has not been observed in TEM micrographs for Pd/Al_2O_3 catalysts as it was observed in [30].

Note that earlier comparable series of Au, Au-Pd and Pd catalysts subjected to activation in oxygen and hydrogen were characterized in detail in [30]. Some additional data obtained by TEM, XPS and UV-vis for these samples can be found there [30].

In the current study, the synthesized catalysts were also characterized by XPS to explore the chemical state of Au and Pd. The XPS spectra for Au 4f, Au 4d and Pd 3d are shown in Figures 4 and 5. The spectra for Pd 3d are characterized with a low intensity while the spectra for Au 4f and Au 4d manifest high intensity due to the difference in the Au and Pd loading. The Au 4f spectra, characterized by the two spin-orbit components, Au $4f_{7/2}$ and Au $4f_{5/2}$ separated by 3.67 eV, exhibit two doublets attributed to Au^o and Au^+ species (according to [32]) only for samples after the oxidative thermal pre-treatment. Spectra deconvolution revealed that the relative content of positively charged gold was equal *c.a.* 6.6 % and 24.9% for pre-oxidized Au/Al_2O_3 and $AuPd/Al_2O_3$, respectively. Only metallic gold species were found for the pre-reduced samples (see Table 2). The Pd 3d spectra characterized by two spin-orbit components, Pd $3d_{5/2}$ and Pd $3d_{3/2}$ separated by 5.26 eV, exhibit only one doublet attributed to Pd^o species according to [32] (Table 3). No traces of positively charged Pd species were found even for pre-oxidized $AuPd/Al_2O_3$ catalyst. Interactions between Au and Pd seem to be efficient enough resulting in the formation Au-Pd solid alloy. It is well known that Pd metallic species well mixed with gold in such alloys are resistant to re-oxidation [30, 33, 34]. Indeed, a slight noticeable shift of the Au$4f_{7/2}$ peak maximum for Au^o species to lower energy for a bimetallic catalyst (Table 3), characteristic for Au-Pd alloys was observed [34]. Such a shift of Au 4f7/2 peak to low energy is usually attributed to formation of highly dispersed gold species. However, according to TEM data $Pd–Au/Al_2O_3$ is characterized with almost the same (TPO) or larger (TPR) gold particles than Au/Al_2O_3. Therefore, this effect similar to the one observed earlier in [35, 36] could be interpreted by electronic interactions between Pd and Au due to formation of the Au–Pd alloy. The latter may explain the presence of only metallic Pd species even for the sample treated in oxygen. A very low Pd content (*ca.* 0.039 atom. %) did not allow acquisition of a reliable Pd XPS spectrum for Pd/Al_2O_3 catalyst and to perform a fair comparison of the state of Pd state in Au-Pd/Al_2O_3 and Pd/Al_2O_3 catalysts.

3.2.Catalytic results

In order to explore the influence of bimetallic interactions on the catalytic performance, gold, gold–palladium, and palladium catalysts activated in oxygen or hydrogen were tested in one-pot myrtenol amination with aniline.

Based on our previous results gold-catalyzed myrtenol amination with aniline led to the predominant formation of myrtenal and its imine (**1**) and amine (**2**) (Figure 2). At the same time depending on the catalysts the hydrogenation of C=C bond as a side process occurred. As a result myrtanol, myrtanal and the corresponding imine (**3**) and amine (**4**) were formed in small amounts in the presence of gold catalysts [3]. Additionally no myrtenol isomerization products were observed in the presence of Au catalysts. Alumina *per se* resulted in the formation of the corresponding imine (**1**) with selectivity of 94% at myrtenol conversion *ca.* 40% after 7 h independent on the support redox activation. To enhance mainly the hydrogen transfer to C=N bond, low amounts of Pd (0.2 wt. %) were introduced to the gold catalyst in the present work. At the same alumina supported Au, Au-Pd and Pd catalysts showed different catalytic behavior in the reaction. The results are presented in Figures 6 and Table 4.

The catalysts demonstrated nearly close catalytic activity within one type of the catalysts activation in terms of myrtenol conversion vs. time decreasing in the following range Au>Au-Pd>Pd and Au-Pd>Au>Pd for pre-oxidized and pre-reduced catalysts, respectively (Figure 6). Taking into account the active metal content in the samples determined by ICP and the metal dispersion (D) estimated from TEM images (Table 1) for metal nanoparticles using formula $D = 8 \cdot r_{Me} / d_{Me}$, where r_{Me} is radius of metal atom(nm) and d_{Me} is particle mean diameter (nm), the initial reaction rates normalized by amount of accessible active metal atoms were calculated (Table 4). As it has been mentioned above deposition of palladium onto gold nanoparticles practically did not affect the size of bimetallic nanoparticles because of a low palladium loading. For AuPd catalysts the TOF value was calculated using TEM data. In the case of monometallic

Pd catalyst it was proposed that all Pd atoms are accessible for the reactants. Assuming each surface atom constitutes an active centre, the TOF can then be given as, $TOF = \frac{n^0_{myrtenol} - n_{myrtenol}}{n_{Me} \cdot D \cdot t}$

where $n^0_{myrtenol}$ and $n_{myrtenol}$ are the initial amount of myrtenol in moles and the molar amount of myrtenol after 1h, n_{Me} (mol) the amount of active metal in the catalyst, D is the dispersion of particles, t is the reaction time (h).

In this case, for the pre-oxidized bimetallic catalyst introduction of Pd did not improve the catalytic activity. Monometallic Pd catalyst was rather active in myrtenol dehydrogenation compared Au-containing catalysts with the initial reaction rate being *ca.* 3.4 fold higher for Pd/Al_2O_3 catalyst. The TOF value for pre-reduced $AuPd/Al_2O_3$ catalyst was close to the monometallic Au catalyst. Within one active metal composition the pre-reduced samples promoted significantly faster myrtenol dehydrogenation being caused by the effect of the catalyst redox activation (Table 4). Such effect of redox activation on catalytic performance was studied in detail in our previous work [4]. Note that according to the plausible reaction mechanism the basic sites on the metal oxide surfaces are required for the initial alcohol activation, while availability of protonic groups was suggested to be important for the desired t amine formation and accumulation of the primary amine on the surface [3]. Pre-reduced catalysts were shown to be more effective in alcohol dehydrogenation due to enhancing of the support basic properties required for the initial alcohol activation [4]. Thermal activation of catalysts in oxygen resulted in a higher efficiency of ammonia removal, formed as a result of decomposition/transformation of compounds used during catalyst preparation (*i.e.* NH_4OH and urea),compared to treatment in hydrogen. Differences in activity and selectivity for pre-reduced and pre-oxidized catalysts were proposed to be mainly related to a different degree of the support basic properties modification by residual ammonia [4].

More noticeable differences in the catalytic behavior for the studied catalysts were seen in selectivity towards the products profoundly affected by the nature of nanoparticles. Selectivity to different groups of the reaction products is presented in Table 4.

Au/Al_2O_3 catalyst was active in the formation of the target amine (**2**) and the corresponding imine (**1**) without a significant impact of the side reaction of C=C bond hydrogenation. Au/Al_2O_3 catalyst treated under an oxidizing atmosphere was more effective in terms of the target secondary amine (**1**) yield. An increase in selectivity to myrtenal for the pre-reduced catalysts was also related to catalyst activation. Myrtenal accumulation in the reaction mixture in the presence of pre-reduced catalysts was caused by a lack of aniline adsorption on the catalysts due to modification of their basic properties affecting eventually selectivity to the target amine. This effect was described in detail in [4]. Thus, the gold catalyst was effective for the hydrogen transfer.

Opposite, in the case of monometallic Pd catalyst the formation of imine (**1**) was observed, whereas the products of hydrogen borrowing reaction to C=N bond were almost not detected and hydrogen produced in the first step was consumed for C=C bond hydrogenation in the initial myrtenol to form myrtanol (Table 4). Selectivity to myrtanol was even higher over the pre-reduced sample compared to the pre-oxidized one most likely due to formation of the trace amounts of non-active palladium oxide film over Pd nanoparticles under pre-treatment in oxygen. Indeed, the formation of palladium oxide film over Pd nanoparticles exposed to oxygen was found in [30].

Bimetallic Au-Pd catalyst despite high activity demonstrated lower selectivity to the target amine (**2**) independently on the type of the catalyst activation. Note, that pre-oxidized Au-Pd catalyst did not promote imines formation and only a small amount of N-containing products was detected in the reaction mixture. Myrtenal accumulation occurred along with C=C bond hydrogenation in myrtenol. Low amount of N-containing products can be explained by a lack of aniline on the catalyst surface as discussed above. Contrary to that, Au-Pd catalyst pre-treatment

in hydrogen did not result in any limitations regarding imine (**1**) formation, while the target amine (**2**) was formed only in a small amount. Both myrtanol and myrtanal were detected in the reaction mixture. Moreover, formation of imine (**3**) and amine (**4**) with the saturated C-C bond was more noticeable compared to monometalic Au and Pd catalysts. Therefore, Au-Pd nanoparticles activate C=C bond rather than C=N one and did not promote hydrogen transfer because of hydrogen consumption for the side C=C bond hydrogenation. Note that formation of imine observed over Pd-containing catalysts can be also of interest. Imines are important intermediates in the synthesis of biologically active N-containing compounds and in industrial synthetic processes [37, 38, 39, 40].

Thus, the first step of one-pot alcohol amination, alcohol dehydrogenation, is promoted on the support basic sites and strongly depends of the support basic properties [3], while hydrogen is further stabilized on active metal and reacting directly with the unsaturated bond activated on the active metal. However, the active metal composition and the support treatment during the catalyst synthesis can affect the surface active sites of the support resulting as well in catalytic activity modification.

Overall, the pre-reduced monometallic Pd catalyst compared to bimetallic Au-Pd was more active in direct myrtenol hydrogenation to myrtanol, while for Au-Pd formation of myrtanal was mainly detected among saturated products containing oxygen. In fact, previously Pd catalysts were shown to be highly effective for C=C bond hydrogenation in α-pinene with a similar structure [11]. On the other hand, pre-oxidized Au-Pd catalyst resulted in myrtenal and myrtanol formation among O-containing products giving limited amounts of imines. A noticeable difference in activity of pre-oxidized and pre-reduced Au-Pd catalysts is proposed to be related to the active phase composition. As it was earlier demonstrated in [30] external surface of bimetalic Au-Pd nanoparticles activated in hydrogen exhibit predominantly well mixed metallic Au-Pd species with a possible formation Au-Pd alloy, while the catalyst pre-oxidation leads to formation of both Au-Pd alloy and PdO species, with the later present most

likely as a thin layer over Au-Pd alloy. Availability of metallic gold species in the case of pre-reduced Au-Pd catalyst seems to result in a more effective hydrogen transfer compared to the pre-oxidized sample. At the same time, formation of myrtanol observed in the presence of pre-oxidized $AuPd/Al_2O_3$ was typical for palladium catalysts independent on the type of the catalyst pre-treatment.

Nevertheless comparison between Au and Pd catalysts revealed that Au catalyst was more active and selective in one-pot alcohol amination for the initial substrates with a reactive unsaturated C=C bond and even promoted hydrogen transfer more effectively. Pd presence resulted in C=C bond activation and its further hydrogenation by hydrogen formed in the first step of alcohol dehydrogenation. At the same time the catalytic activity of palladium catalyst with a low active metal content (0.2 wt. %) is higher than Au-containing catalyst. In this case Pd catalysts seems to be effective for the substrates with a less complicated structure when there is no need to avoid side reactions, in particular C=C bond hydrogenation. A similar result was observed for Pd/MgO catalyst by Corma *et al.* [41], who showed that Pd catalysts were active for benzyl alcohol amination with aniline catalyzing on the other hand the final step of C=N bond hydrogenation with a significantly lower chemoselectivity for the substrates containing a nonconjugated C=C bond. These palladium catalysts [27] even did not promote hydrogen transfer for the imine bond in the presence of a conjugated C=C bond. In the current work introduction of Pd to Au nanoparticles even in a small amount resulted in simultaneous hydrogenation of both C=C and C=N bonds.

4. Conclusions

The regularities of one-pot terpene alcohol amination were studied in the presence of Au, Au-Pd and Pd nanoparticles supported on alumina and subjected to activation in oxygen or hydrogen. The effect of the active metal composition on catalytic performance was investigated with biomass derived terpene alcohol (myrtenol), containing different functional groups. Selectivity to the target product (amine) as well as the products of side reactions could serve a descriptor of catalytic behavior in addition to activity evaluation. The synthesized catalysts were studied in detail by TEM, XPS, ICP and nitrogen adsorption.

A noticeable effect of the active metal on selectivity was observed. Monometallic Au/Al_2O_3 catalyst promoted predominantly formation of the target secondary amine and the corresponding imine without a significant impact of the side reaction of C=C bond hydrogenation in myrtenol. Bimetallic Au-Pd catalyst despite its high activity demonstrated lower selectivity to the target amine due to occurrence of the side C=C bond hydrogenation making the products formation non-selective. Au-Pd nanoparticles activate C=C bond rather than C=N one and did not promote hydrogen transfer because of hydrogen consumption for the side C=C bond hydrogenation. For Pd catalyst hydrogenation of the C=C bond in myrtenol occurred selectively without hydrogen transfer to C=N bond. Monometallic Pd catalyst was mainly characterized by formation of myrtanol and imine. The active metal thus determines selectivity of hydrogen transfer. Hydrogen produced in the first step of alcohol dehydrogenation reacts directly with the unsaturated bond activated on the active metal. Pd presence resulted in C=C bond activation and its further hydrogenation, while Au promoted C=N bond hydrogenation. Nevertheless, utilization of Pd-containing catalyst can be justified for the substrates with a less complicated structure without competitive unsaturated groups due to noticeably higher activity.

Acknowledgements

The authors acknowledge the technical assistance of E. Smolentseva, E. Flores, P. Casillas, F. Ruiz, E. Aparicio and J. Peralta.

This work was supported by Ministry of Science and Higher Education of the Russian Federation (project AAAA-A17-117041710075-0).

Compliance with Ethical Standards

Conflict of interest. All authors claim no conflict of interest.

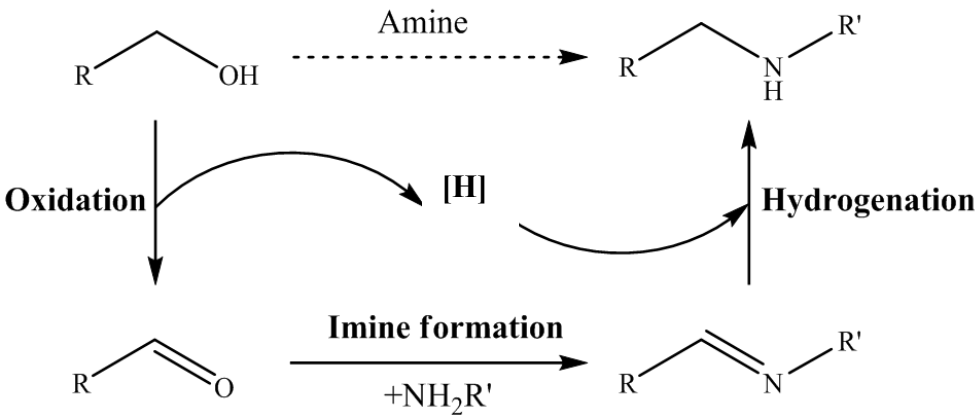

Fig. 1. General scheme of the one-pot alcohols amination.

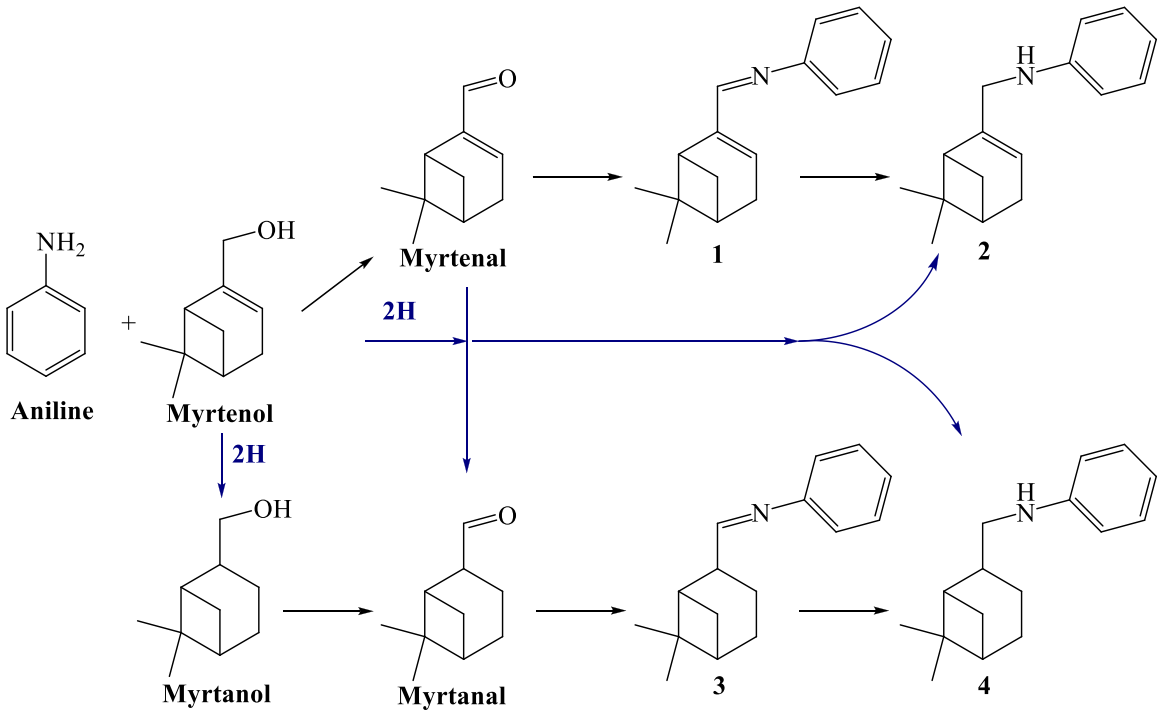

Fig. 2. Scheme of myrtenol amination with aniline over Au catalysts.

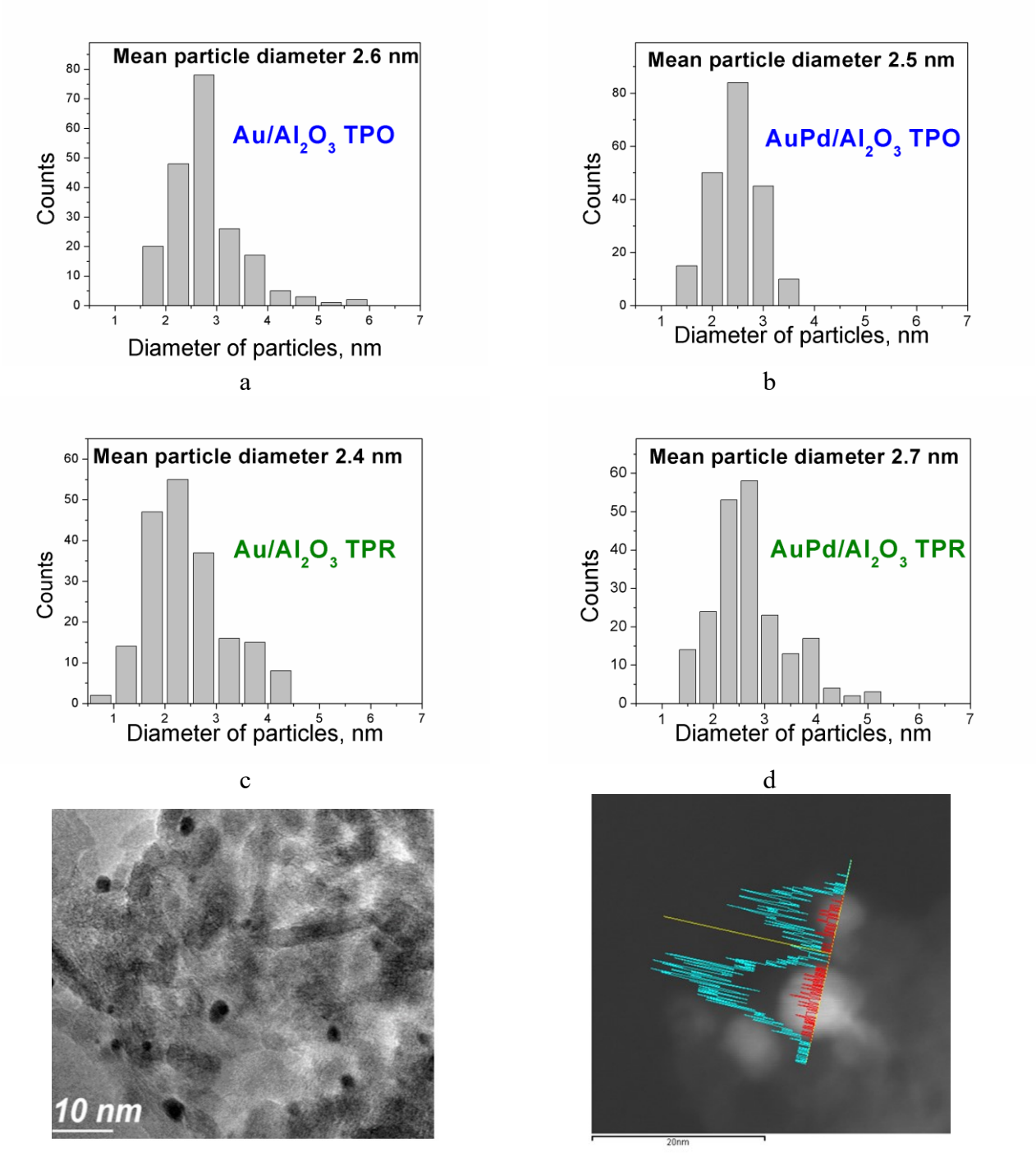

Fig. 3. Particle size distribution according to TEM analysis for Au/Al_2O_3 (first column), $AuPd/Al_2O_3$ (second column) after TPO (a, b) and TPR (c, d). Typical TEM micrograph for Au/Al_2O_3 sample after TPR (e) and profiles of Au (blue) and Pd (red) across an Au-Pd nanoparticle according to STEM-EDS line scanning technique for $Au\text{-}Pd/Al_2O_3$ sample after TPR (f).

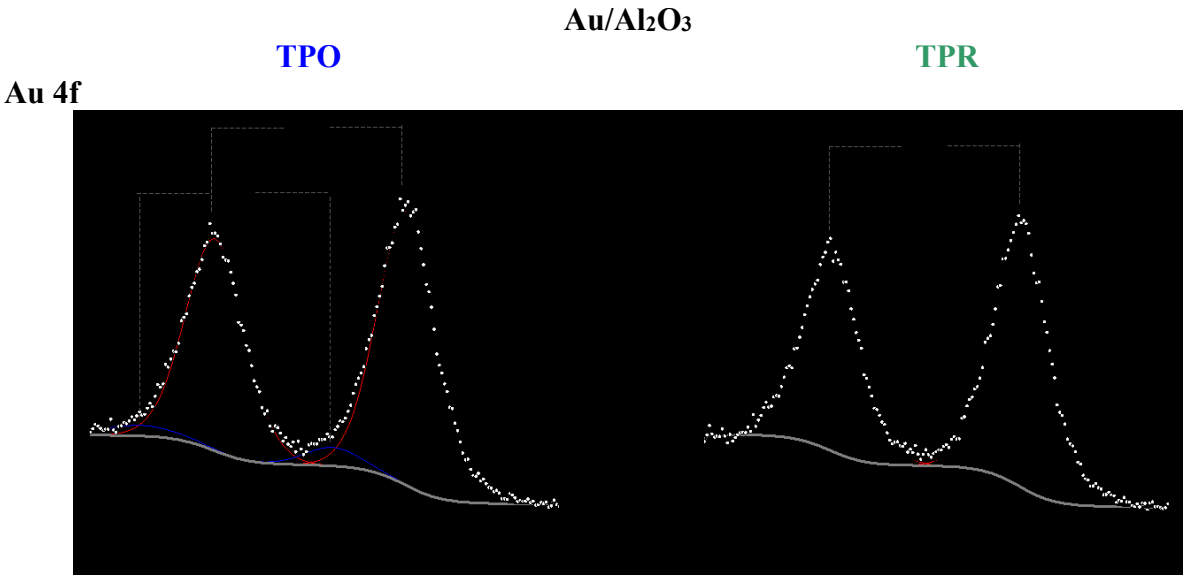

Fig. 4. XPS Au 4f spectra of Au/Al_2O_3 TPO (left) and TPR (right) catalysts (symbols – experimental data, curves – fitting).

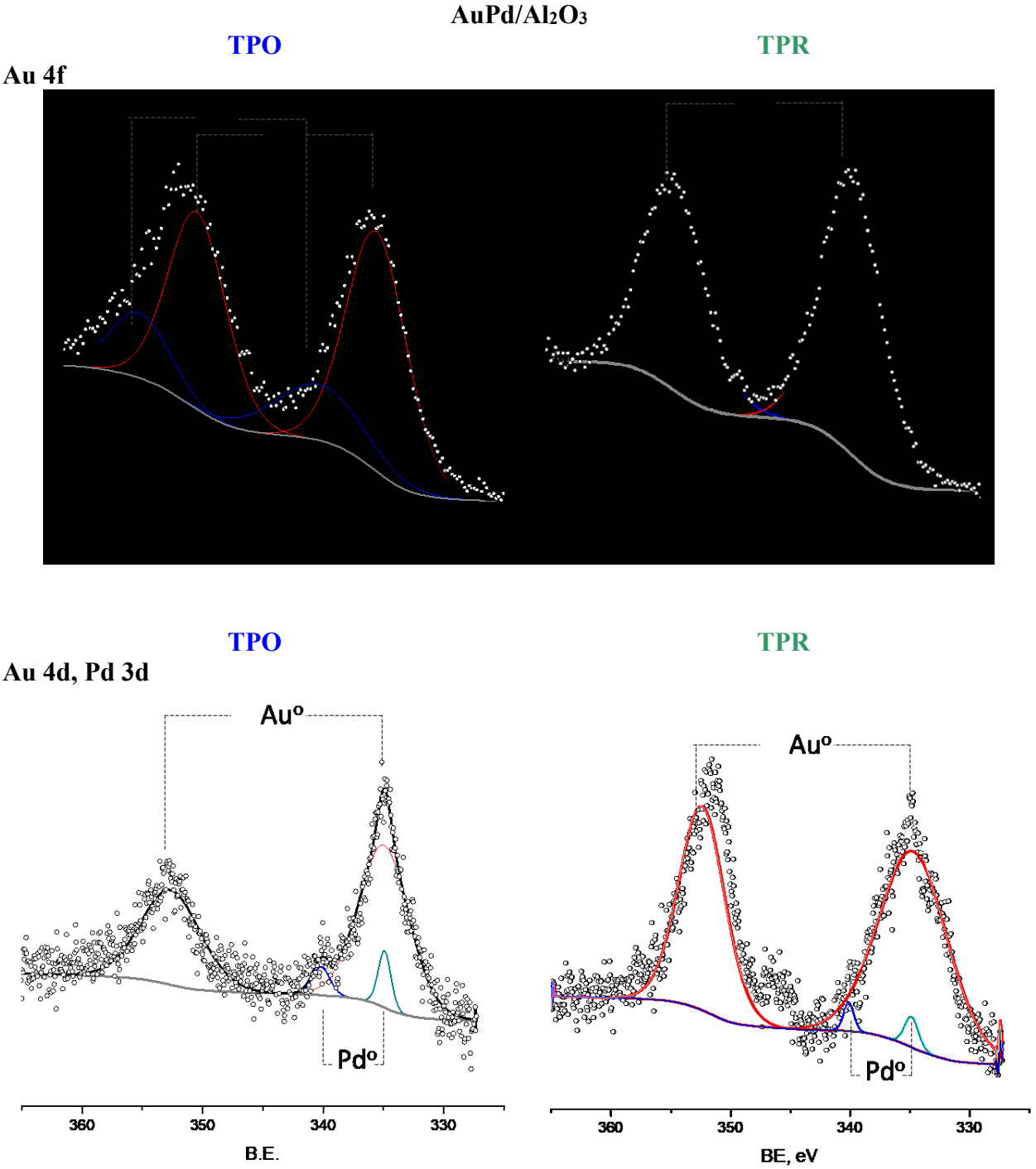

Fig. 5. XPS Au 4f (first row) and Au 4d, Pd 3d (second row) spectra for $AuPd/Al_2O_3$ TPO (left) and TPR (right) catalysts (symbols – experimental data, curves – fitting).

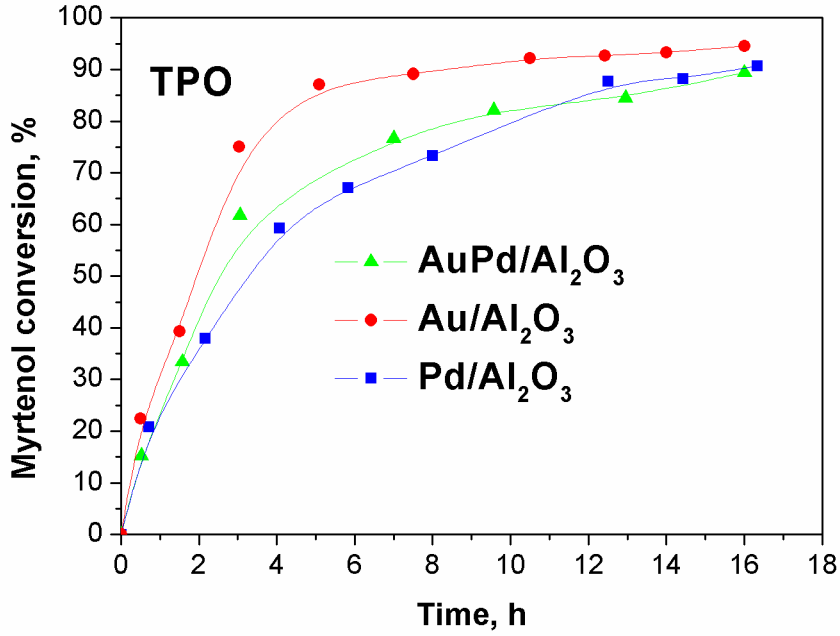

a

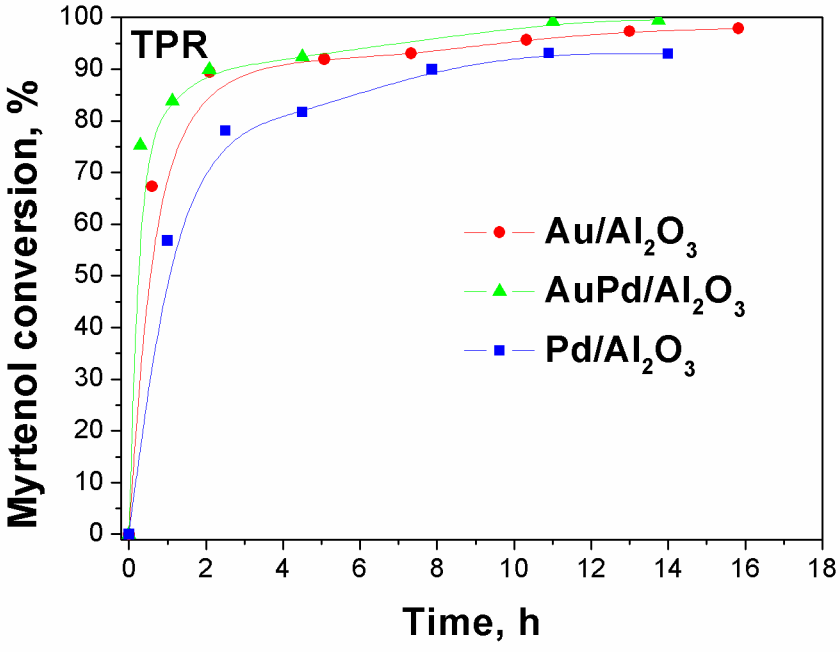

b

Fig. 6. The effect of catalyst active metal and redox treatment on myrtenol conversion in the presence of Au, Au-Pd, Pd supported on Al_2O_3 pre-treated in oxygen (TPO, a) or hydrogen (TPR, b). The reaction conditions: T = 180°C, myrtenol 1 mmol, aniline 1 mmol, toluene 10 ml, catalyst 92 mg.

Table 1. TEM and ICP data for Au, Au-Pd and Pd catalysts.

Catalyst	Metal content, wt.%		Mean particle diameter, nm	
	Au	Pd	TPO[a]	TPR[a]
Au/Al_2O_3	2.3	0	2.6 ± 0.8	2.4 ± 0.7
$AuPd/Al_2O_3$	2.8	0.2	2.5 ± 0.5	2.7 ± 0.7
Pd/Al_2O_3	-	0.2	-	-

[a]Preliminary catalysts activation.

Table 2. Relative content of Pd and Au species in samples after different treatments according to XPS analysis.

Sample	Type of treatment			
	TPO		TPR	
	Au $4f_{5/2}$	Pd $3d_{5/2}$	Au $4f_{5/2}$	Pd $3d_{5/2}$
Au/Al_2O_3	Au^0 (93.4) Au^+(6.6)		Au^0 (100)	
$Pd\text{-}Au/Al_2O_3$	Au^0 (75.1) Au^+ (24.9)	Pd^0 (100)	Au^0 (100)	Pd^0 (100)

Table 3. XPS data of Au 4f, Pd 3d binding energies values, eV referred to as C 1s (284.8 eV) for studied samples.

Sample	Type of sample pretreatment			
	TPO		TPR	
	$Au4f_{7/2}$	$Pd3d_{5/2}$	$Au4f_{7/2}$	$Pd3d_{5/2}$
Au/Al_2O_3	Au^o(83.9; 1.2) Au^+(85.3;1. 4)	-	Au^o(83.9;1.2)	-
$AuPd/Al_2O_3$	Au^o(83.7; 1.4) Au^+(84.8; 1.7)	Pd^o(334.9; 1.3)	Au^o(83.5; 1.4)	Pd^o(334.8; 1.2)

In parentheses the peak position of Pd and Au species and the full width at half maximum (FWHM) are shown

Table 4. Initial normalized reaction rate and selectivity to the products at the same value of myrtenol conversion (85%) for myrtenol amination in the presence of Au, Au-Pd, Pd supported on Al_2O_3 pre-treated in oxygen (TPO) or hydrogen (TPR). The reaction conditions: T = 180°C, myrtenol 1 mmol, aniline 1 mmol, toluene 10 ml, catalyst 92 mg.

Catalyst	TOF[b], h^{-1}	Selectivity, %[c]						
		myrtenal	myrtanol	myrtanal	1	2	3	4
TPO[a]								
Au/Al_2O_3	67	6	12	6	40	31	1	3
$AuPd/Al_2O_3$	38	50	25	7	8	2	3	4
Pd/Al_2O_3	129	26	31	2	32	2	3	2
TPR[a]								
Au/Al_2O_3	137	26	12	5	35	19	1	1
$AuPd/Al_2O_3$	143	8	9	20	36	7	8	10
Pd/Al_2O_3	294	21	46	1	27	2	1	1

[a]Preliminary catalysts activation;
[b]Turnover-frequency was calculated after 1 h;
[c]Selectivity to the reaction products presented in Figure 2.

References

[1] Demidova YuS, Suslov EV, Simakova IL, Mozhajcev ES, Korchagina DV, Volcho KP, Salakhutdinov NF , Simakov AV, Murzin DYu (2017) J Mol Catal 426:60-67

[2] Demidova YuS, Suslov EV, Simakova IL, Volcho KP, Smolentseva E, Salakhutdinov NF, Simakov AV, Murzin DYu (2017) J Mol Catal 433:414-419

[3] Demidova YuS, Simakova IL, Estrada M, Beloshapkin S, Suslov EV, Korchagina DV , Volcho KP, Salakhutdinov NF, Simakov AV, Murzin DYu (2013) Appl Catal A: Gen 464-465:348-356

[4] Simakova IL, Demidova YuS, Estrada M, Beloshapkin S, Suslov EV, Volcho KP, Salakhutdinov NF, Murzin DYu, Simakov AV (2017) Catal Tod 279:63-70

[5] Simakova IL, Simakov AV, Murzin DYu (2018) Catalysts 8:365 (1-36).

[6] Kapitsa IG, Suslov EV, Teplov GV, Korchagina DV, Komarova NI, Volcho KP, Voronina TA, Shevela AI, Salakhutdinov NF (2012) Pharm Chem J 46(5):263-265

[7] Tolstikova TG, Morozova EA, Pavlova AV, Bolkunov AV, Dolgikh MP, Koneva EA, Volcho KP, Salakhutdinov NF, Tolstikov GA (2008) Dokl Chem 422(2):248–250

[8] Park DI, Kim HG, Jung WR, Shin MK, Kim KL, Neuropharmacology, 61 (2011) 276-282

[9] Silver AA, Shytle RD, Sheehan KH, Sheehan DV, Ramos A, Sanberg PR (2001) J Am Acad Child Adolesc Psychiatry 40:1103–1110

[10] Il'ina IV, Volcho KP, Salakhutdinov NF (2008) Russian Journal of Organic Chemistry 44:1-23

[11] Simakova IL, Solkina Yu, Deliy I, Wärnå J, Murzin DYu (2009) Appl Catal A: Gen 356:216-224

[12] Solkina YuS, Reshetnikov S, Estrada M, Simakov AV, Murzin DYu, Simakova IL (2011) Chem Eng J 176-177:42-48

[13] Costa V V, Estrada M, Demidova Y, Prosvirin I, Kriventsov V, Cotta R F, Fuentes S, Simakov A, Gusevskaya E V (2012) J Catal 292:148-156

[14] Ravasio N, Zaccheria F, Guidotti M, Psaro R (2004) Top Catal 27:1-4

[15] Demidova YuS, Suslov EV, Simakova OA, Simakova IL, Volcho KP, Salakhutdinov NF, Murzin DYu (2015) Catal Tod 241:189–194

[16] Demidova YuS, Simakova IL, Wärnå J, Simakov AV, Murzin DYu (2014) Chem Eng J 238:164-171

[17] Semikolenov VA, Ilyna II, Simakova IL (2001) Appl Catal A Gen 211: 91-107

[18] Ancel JE, Maksimchuk NV, Simakova IL, Semikolenov VA (2004) Appl Catal A Gen 272: 109-114

[19] Semikolenov VA, Ilyna II, Simakova IL (2002) J Mol Catal A Chem182-183: 383-393

[20] Demidova YuS, Suslov EV, Simakova IL, Mozhajcev ES, Korchagina DV, Volcho KP, Salakhutdinov NF, Simakov AV, Murzin DYu (2018) J Catal 360: 127–134

[21] Ishida T, Takamura R, Takei T, Akita T, Haruta M (2012) Appl Catal A: Gen 413-414:261-266

[22] Ishida T, Kawakita N, Akita T, Haruta M (2009) Gold Bull 42:267–274

[23] Zaytseva YuA, Panchenko VN, Simonov MN, Shutilov AA, Zenkovets GN, Simakova IL, Parmon VN (2013) Top Catal 56: 846-855

[24] Shimizu K, Nishimura M, Satsuma A (2009) ChemCatChem 1:497–503

[25] Mäki-Arvela P, Kuusisto J, Mateos Sevilla E, Simakova IL, Mikkola J-P, Myllyoja J, Salmi T, Murzin DYu (2008) Appl Catal A Gen 345: 201-212

[26] Mäki-Arvela P, Martin G, Simakova IL, Tokarev A, Wärnå J, Hemming J, Holmbom B, Salmi T, Murzin DYu (2009) Chem Eng J 154: 45-51

[27] Simakova OA, Simonov PA, Romanenko AV, Simakova IL (2008) React Kinet Catal Lett 95: 3-12

[28] Martinez-Ramirez Z, Gonzalez-Calderon JA, Almendarez-Camarillo A, Fierro-Gonzalez JC (2012) Surf Science 606 (15-16):1167-1172

[29] Conzales-Yañez EO, Fuentes GA, Hernández-Terán ME, Fierro-Gonzalez JC (2013) Appl Catal A 464-465:374-383

[30] Smolentseva E, Kusema BT, Beloshapkin S, Estrada M, Vargas E, Murzin DY, Castillon F, Fuentes S, Simakov A (2011) Appl Catal A 392:69-79

[31] Ivanova S, Pitchon V, Zimmermann Y, Petit C (2006) Appl Catal A 298:57-64

[32] Moulder JF, Stickle WF, Sobol PE, Bomben KD, Handbook of X-rayPhotoelectron Spectroscopy, Perkin-Elmer Corporation, Physical ElectronicsDivision, Eden Prairie, 1992 p 179

[33] Varga P, Hetzendorf G (1985) Surf Sci 162:544-549

[34] Barbieri PF, Siervo A de, Carazzolle MF, Landers R, Kleiman GG (2004) J Electron Spectrosc 135:113-118

[35] Bond GC, Thompson DT (1999) Catal Rev Sci Eng 41:319–388

[36] Marx S, Baiker A (2009) J Phys Chem C 113:6191–6201

[37] Patil RD, Adimurthy S (2013) Asian J Org Chem 2 (9):726-744

[38] Zakharenko AL, Mozhaitsev ES, Suslov EV, Korchagina DV, Volcho KP, Salakhutdinov NF, Lavrik OI (2018) Chem Nat Comp 54:672-676

[39] Zakharenko A, Luzina O, Koval O, Nilov D, Gushchina I, Dyrkheeva N, Svedas V, Salakhutdinov N, Lavrik O (2016) J Nat Prod 79:2961-2967

[40] Sokolova AS, Yarovaya OI, Baev DS, Shernyukov AV, Shtro AA, Zarubaev VV, Salakhutdinov NF (2017) Eur J Med Chem 127: 661-670

[41] Corma A, Ródenas T, Sabater MJ (2010) Chem Eur J 16:254-260